Supporting Information

Unravelling the promoting effect of ultrathin TaC/RGO nanosheets hybrid for enhanced catalytic activity of Pd nanoparticles

Chunyong He*[a,b], Juzhou Tao*[a,b], Guoqiang He[c] Pei Kang Shen*[c] Yongfu Qiu[d]

Dr. C. He, Prof. J. Tao, Prof. G. He, Prof. P. K. Shen

[a] Institute of High Energy Physics, Chinese Academy of Sciences (CAS), Beijing 100049, China

[b] Dongguan Neutron Science Center, Dongguan 523803, China

[c] Collaborative Innovation Center of Sustainable Energy Materials, Guangxi University, Nanning, Guangxi, 530004, PR China

[d] College of Chemistry and Environmental Engineering, Dongguan University of Technology, Guangdong 523808, P. R. China

E-mail: taoj@ihep.ac.cn (J. Tao); hechunyong@ihep.ac.cn (C. He); pkshen@gxu.edu.cn (P.K. Shen)

Keywords: Two-Dimensional, Transition Metal Carbides, Pd nanoparticles, Methanol oxidation reaction, Direct methanol fuel cells
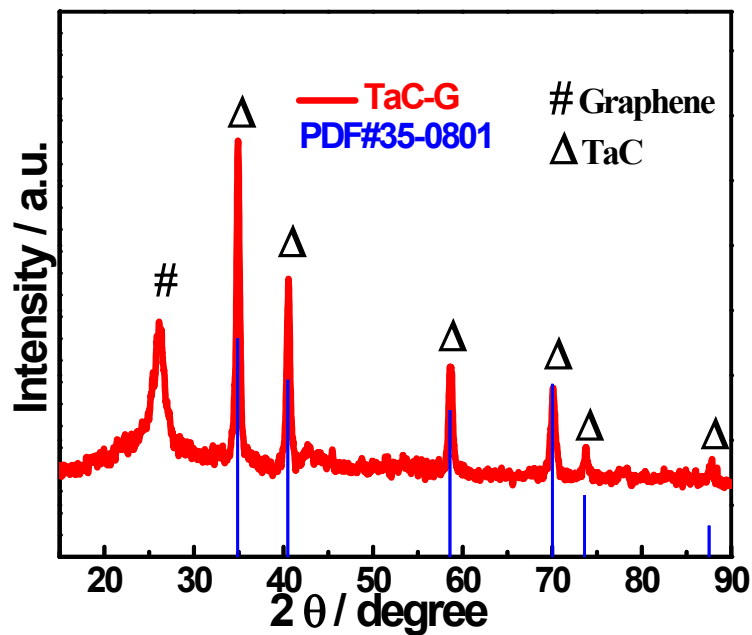
Fig. S1 The XRD pattern of TaC-G. The diffraction peak at $2\theta = 26.2°$ is the characteristic of the graphite (002) plane, demonstrating the reduce of the GO after annealing. The distinct diffraction peaks at $2\theta= 34.94°$, $40.58°$, $58.74°$, $70.12°$, $73.76°$ and $87.86°$ are indexed as the (111), (200), (220), (311), (220), (400) planes of TaC (Cubic, Fm-3m(225)). The blue vertical lines indicate the peaks of the cubicTaC reflections (PDF#35-0801)
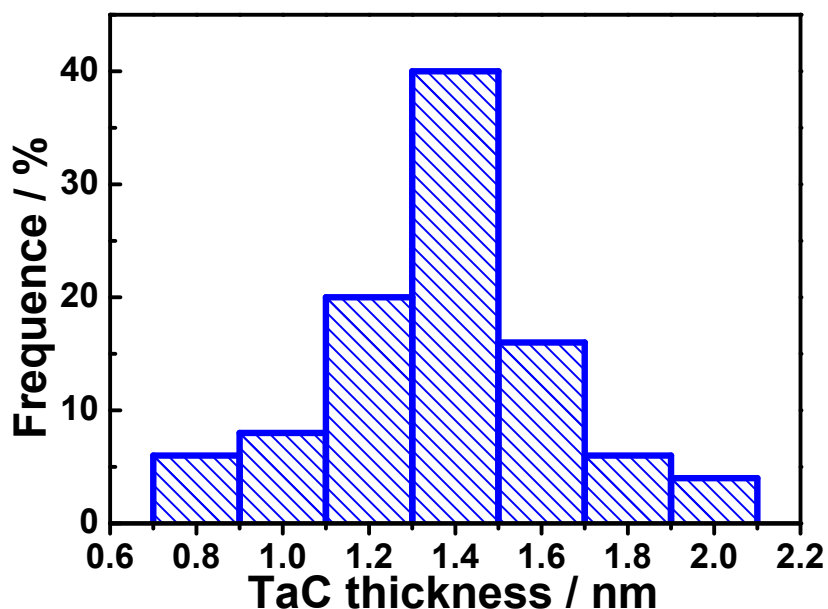

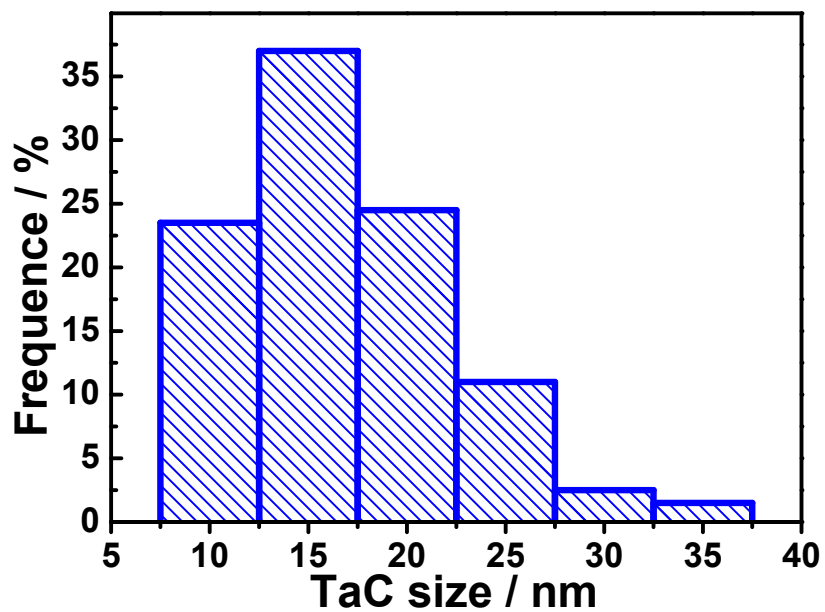**Fig. S2** The thickess distribution histograms of the ultrathin TaC nanosheets.

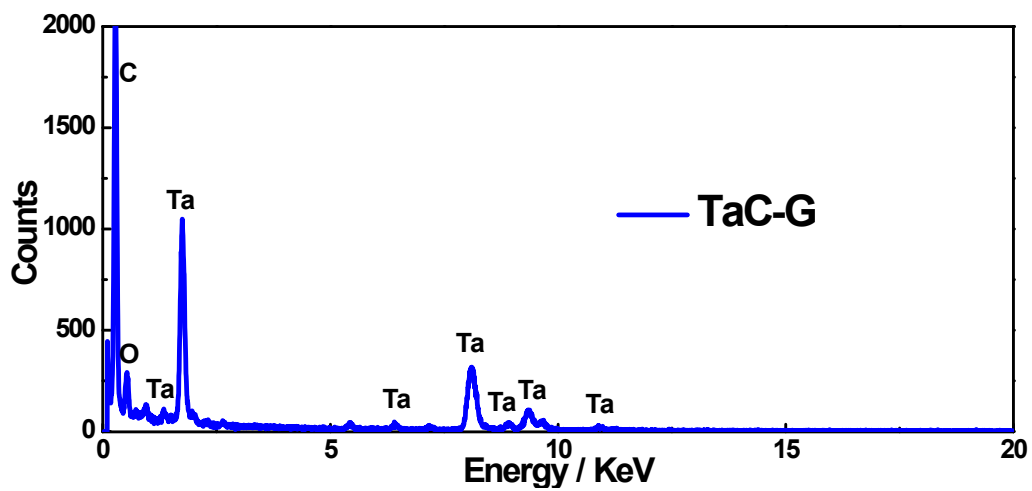**Fig. S3** Size distribution histograms of the ultrathin TaC nanosheets.

Fig. S4 The EDS pattern of TaC-G, showing the coexist of carbon, oxygen and tantalum elements.
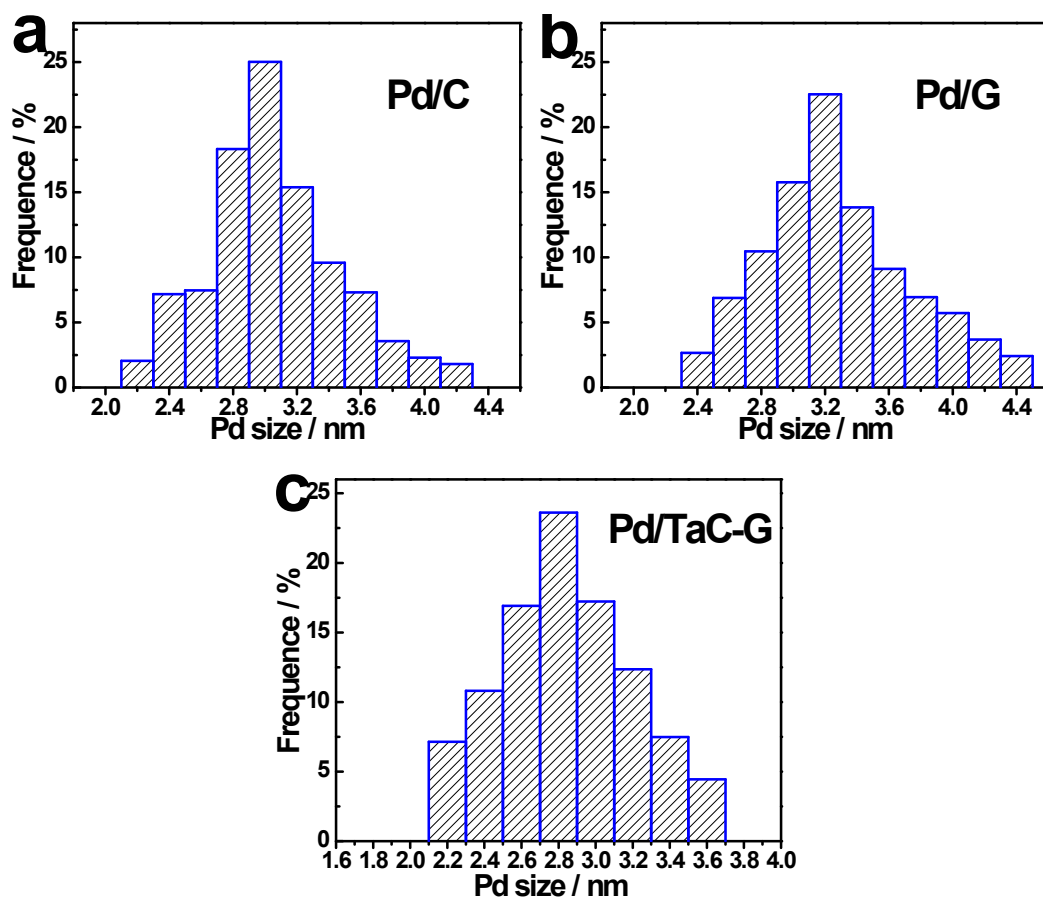
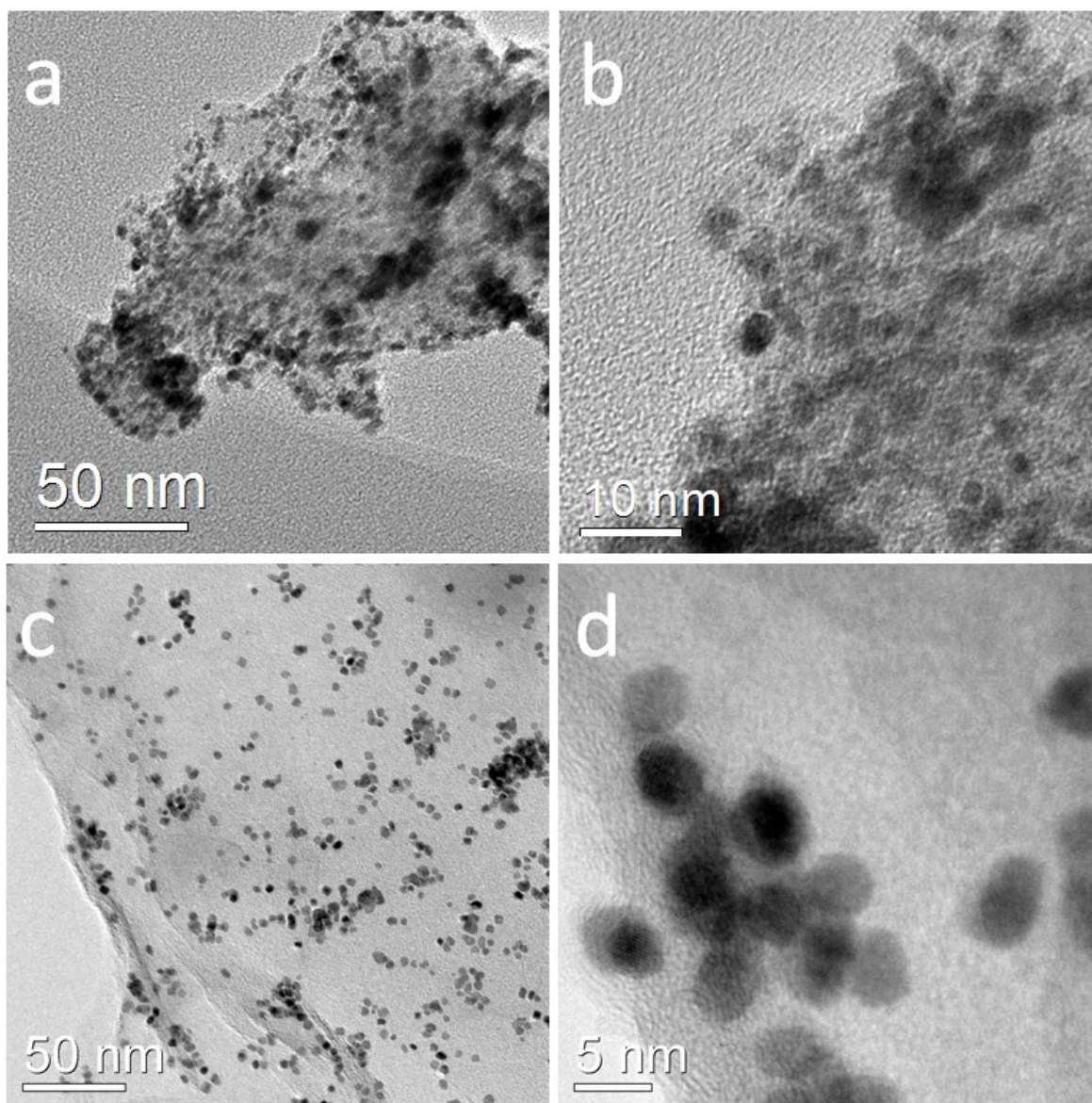**Fig. S5** Size-distribution histograms of the Pd/C (a), Pd/G (b) and Pd/Ta-G (c).

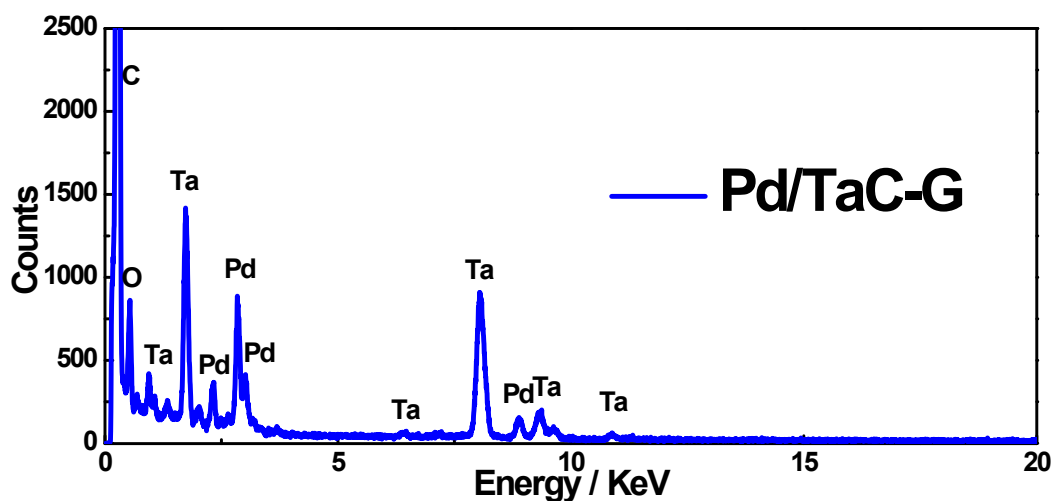**Fig. S6** (a,b) TEM images of Pd/C, (c,d) TEM images of Pd/G,

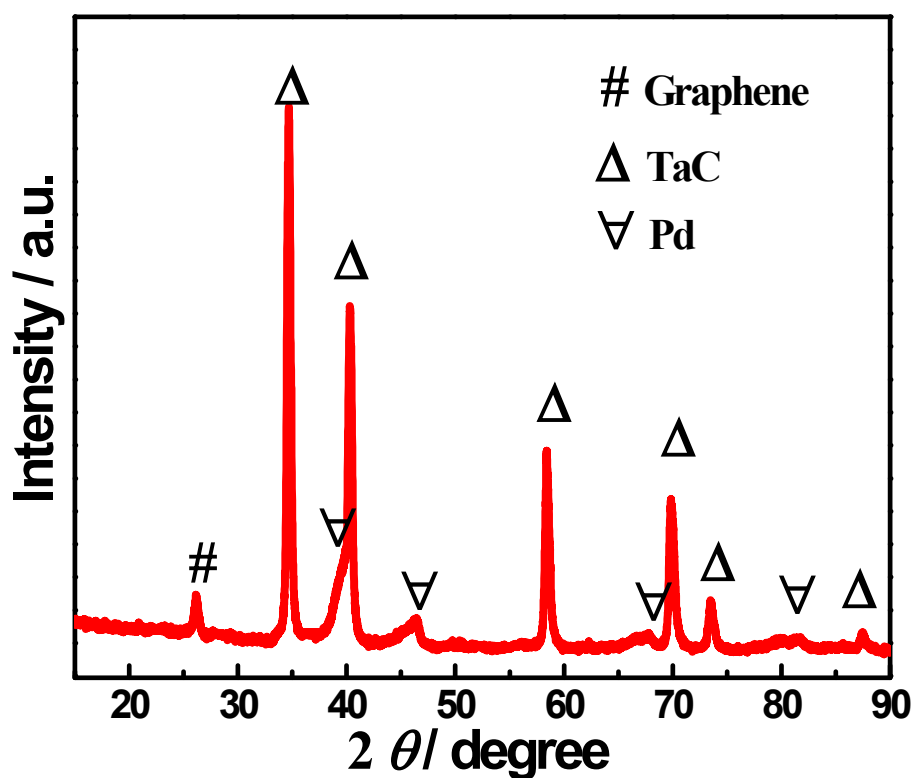**Fig. S7** The EDS pattern of Pd/TaC-G, showing the coexist of carbon, oxygen, tantalum and palladium elements.

Fig. S8 The XRD pattern of Pd/TaC-G, showing the Pd and TaC phases unambiguously. The peaks at 2θ of 40.06°, 46.23°, 67.83° and 81.67° correspond to the (111), (200), (220) and (311) facets of Pd, showing a typical face-centered cubic (fcc) structure.
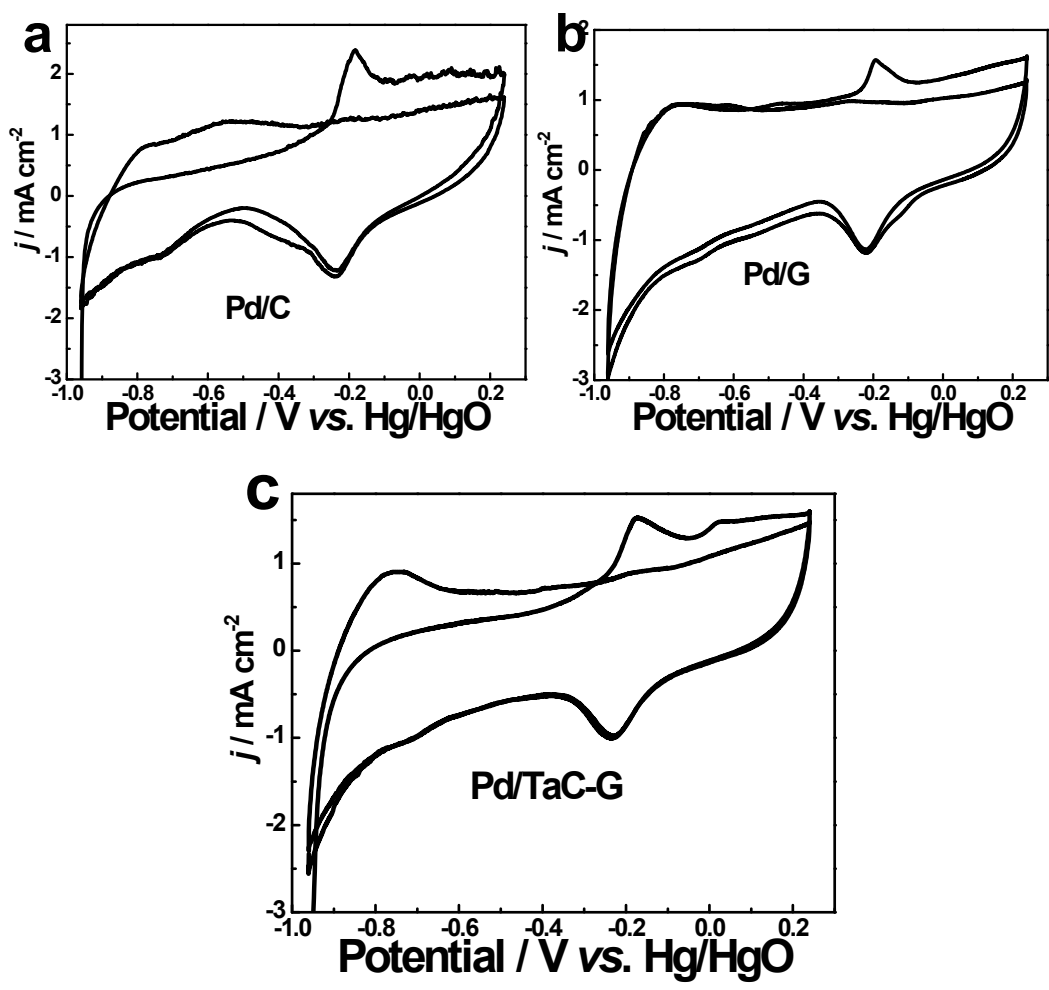
Fig. S9 CO-stripping of Pd/C, Pd/TaC-G and Pd/TaC-G in 1.0 mol L^{-1} KOH solution of Pd/C (a), Pd/G (b) and Pd/TaC-G (c).
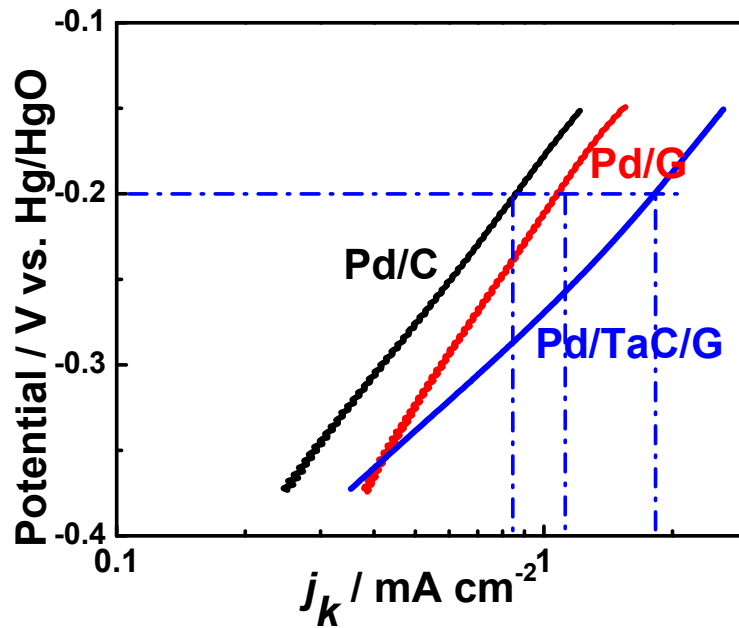
Fig. S10 shows the comparison of specific activities (j_k, calculated from normalizing the electrode current to the ECSA that obtained from the CO stripping) of Pd/C, Pd/G and Pd/TaC-G. The Pd/TaC-G (1.81 mA cm^{-2}) exhibits about 2.1-fold and 1.7-fold enhancement in specific activity compared to that of Pd/C (0.85 mA cm^{-2}) and Pd/G (1.08 mA cm^{-2}) at -0.2 V (*vs.* Hg/HgO), respectively.
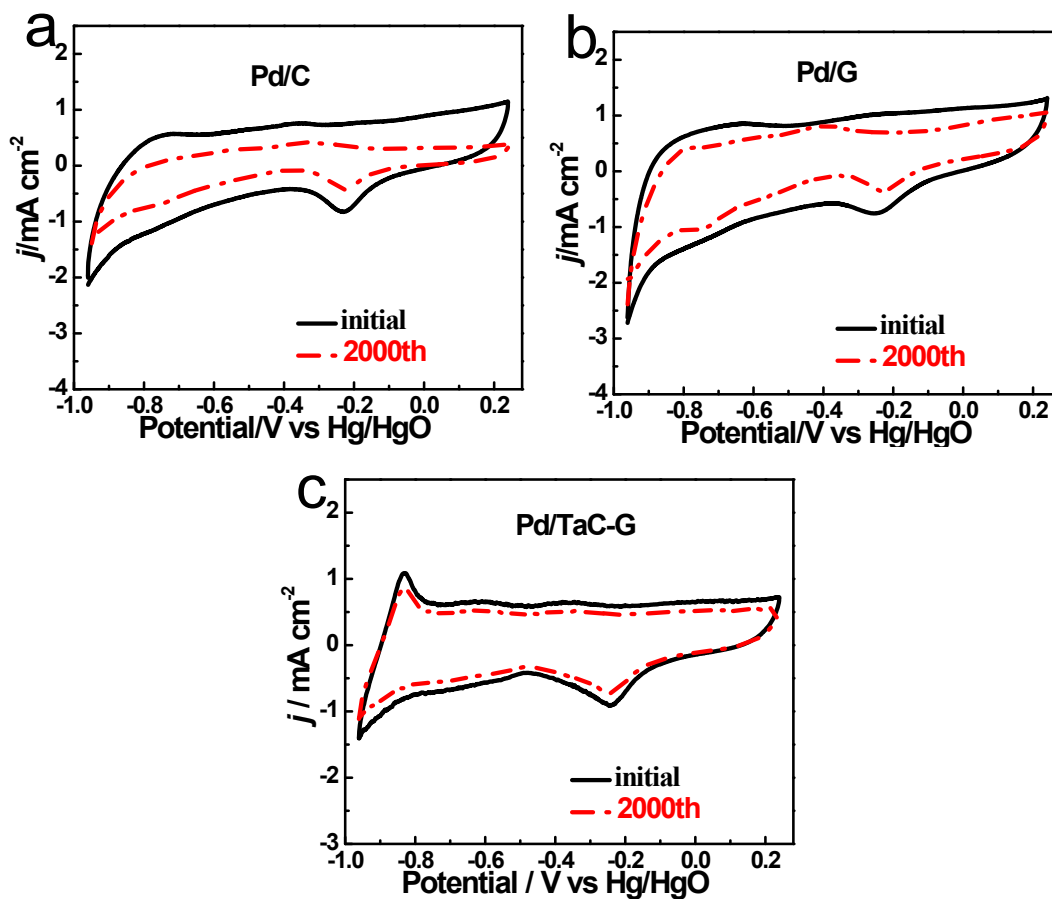
Fig. S11 CVs of Pd/C (a), Pd/G (b) and Pd/TaC-G (c) catalysts before and after the continuous cycling test in N_2-saturated in 1.0 mol L^{-1} KOH solution.
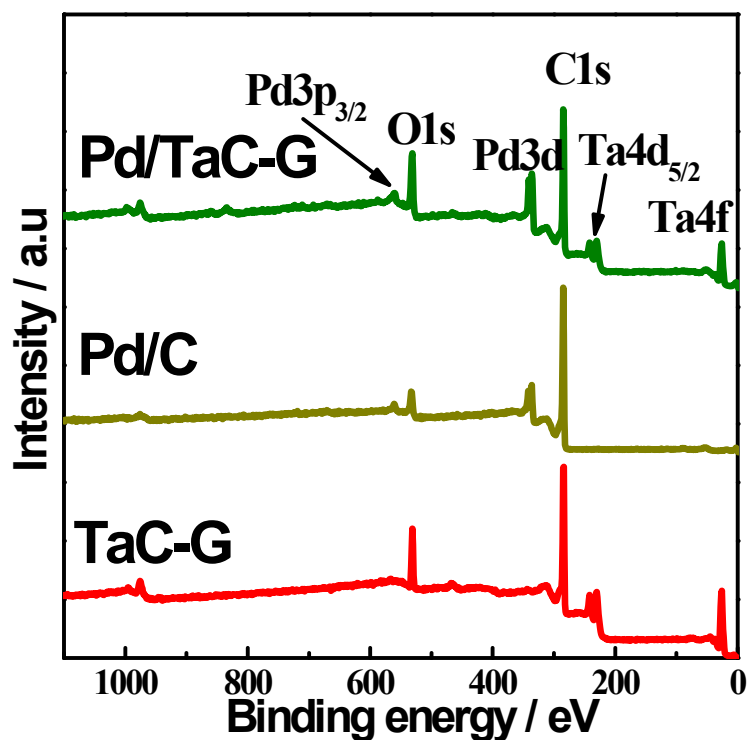
Fig. S12 XPS spectra of the TaC-G, Pd/C and Pd/TaC-G.